Ledge behavior and strength of short-span L-shaped beams

Mohamed K. Nafadi, Omar M. Khalafalla, Gregory W. Lucier, Sami Rizkalla, Paul Zia, and Gary J. Klein

- This paper presents the findings of the first phase of a comprehensive experimental program conducted with the objective of developing design guidelines for the ledges of L-shaped beams that do not overestimate the ledge punching-shear capacity.
- Research findings indicate that even with low levels of global stress, the ledge design procedure provided in the seventh edition of the *PCI Design Handbook: Precast and Prestressed Concrete* could overestimate the ledge capacity.
- The study found that several parameters affected the ledge capacity but are not considered by the PCI procedure.

Precast concrete L-shaped spandrel beams are commonly used in parking structures to support deck members such as double-tee beams. The ledge is cast at the bottom of one face of the web to transfer the eccentric loads from the stems of the double-tee beams resting on the ledge. The L-shaped spandrel beams are simply supported by column haunches or corbels and are connected laterally to the columns to prevent out-of-plane rotation. The deck members are typically connected to the inner surface of the web to limit the lateral displacements of the spandrel beam. The eccentric concentrated loads from the double-tee stems cause both vertical and lateral deflections, as well as rotations of the spandrel beam.

If the applied concentrated loads are sufficiently large, they may cause the ledge to fail in punching shear. Such a failure is usually brittle and is accompanied by localized, wide, diagonal cracks that develop quickly. The exact shape of the failure surface depends on the location of the load within the span of the spandrel beam.

The design procedure for ledges included in the seventh edition of the *PCI Design Handbook: Precast and Prestressed Concrete*,[1] which is called the PCI procedure in this paper, assumes 45-degree failure planes developing from the edges of the bearings. These inclined failure planes are then idealized as rectangular design surfaces for calculating the punching-shear strength of the ledge. **Figure 1** shows the geometry and reinforcement of a typical L-shaped beam ledge, as well as the potential punching-shear failure surface of the

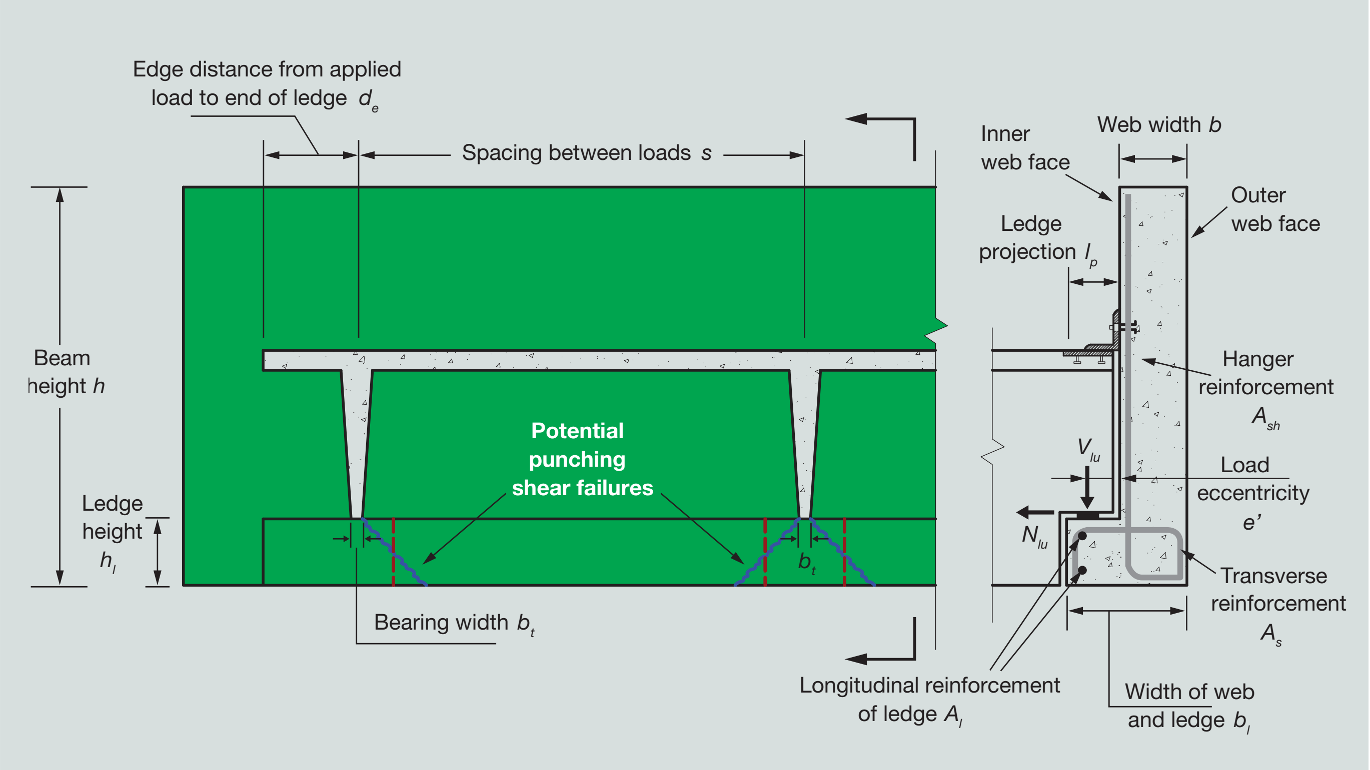

Figure 1. Geometry and reinforcement of a typical ledge of L-shaped beam.
Source: Adapted from the seventh edition of the *PCI Design Handbook: Precast and Prestressed Concrete* (Chicago, IL: PCI, 2010), p. 5–69, Fig. 5.5.1.
Note: N_{lu} = factored ledge friction load; V_{lu} = factored ledge vertical load.

ledge assumed by the PCI procedure. To date, the authors are not aware of any ledge failures due to punching shear; however, several laboratory tests and finite element models have shown that the PCI procedure can sometimes overestimate ledge capacity. In certain cases, particularly those with heavy loading such as green roofs or mixed occupancies, the safety margin provided by the PCI procedure can become questionable. Therefore, a need exists to develop a practical procedure to predict more accurately the ledge capacity of L-shaped spandrel beams.

Klein[2,3] documented three ledge failures in the full-scale testing of three prestressed concrete specimens: two L-shaped beams and one pocket spandrel beam. An unexpected result of the research was the premature punching-shear failures that occurred in the second L-shaped specimen: one near the end and one at an inner location. The primary conclusion from these observed failures was that the PCI procedure significantly overestimated the failure loads measured at both locations. Klein pointed out that the PCI procedure does not consider the effect of load eccentricity or the effect of global flexural and shear stresses (stresses acting on the cross section from beam behavior) on the punching-shear capacity of the ledge.

Hassan[4] conducted a nonlinear finite element analytical study on the punching-shear capacity of L-shaped beam ledges. He used Klein's second L-shaped specimen to calibrate his finite element model to ensure that the program properly simulated the behavior reported by Klein. Hassan then conducted a parametric study consisting of 14 cases to investigate different parameters that were believed to affect the punching-shear capacity of the ledge. The study concluded that the PCI procedure overestimates the ledge capacity, and Hassan recommended a strength reduction factor of 0.60 to provide an adequate safety margin for the punching-shear capacity of the ledge.

Lucier et al.[5–7] conducted an extensive experimental program on 16 full-scale spandrel beams: 13 L-shaped beams and 3 corbeled spandrel beams. The main objective of the research was to develop a rational design methodology for slender spandrel beams. Seven punching-shear failures of the ledge were observed in five of the tested specimens. All measured failure loads were less than those predicted by the PCI procedure. The results also demonstrated that the global stresses in the beam affect the punching-shear capacity of the ledge.

In a discussion of the ledge failures reported by Klein and Lucier, Logan[8] evaluated the test results using the equations provided by the PCI procedure. As an interim precautionary measure, Logan recommended a 50% reduction factor be applied to the capacities predicted by the PCI procedure. Logan also highlighted the need for a research program focused on the punching-shear capacity of the ledges.

A recently completed, comprehensive PCI-funded research program was aimed at the development of practical and reliable design guidelines to predict the punching-shear capacity of the ledges of L-shaped beams. The research was initiated with three-dimensional nonlinear finite element modeling that was calibrated to experimental data obtained from the literature. Using the calibrated finite element models, numerous cases were tested numerically to evaluate the significance of several design parameters believed to affect ledge behavior. Based on the results of the analytical study, a comprehensive experimental program was proposed to better understand ledge behavior under the effect of selected parameters, as well as the configuration of the failure surfaces. The report by Rizkalla et al.[9] provides a full description of the entire research program.

This paper presents the findings of the first phase of this comprehensive research program. In this first phase, short-span beams were chosen to study the punching strength of the ledges under minimal global stress. Using short beams in the experimental program also reduced the cost of each test, thus allowing a larger number of parameters to be tested experimentally. The main objectives of this first-phase study were to investigate the following:

- the ledge behavior at different locations along the beam
- the configuration of the failure surface
- the effects of various parameters believed to have an impact on ledge behavior
- the effectiveness of special reinforcement details

The effect of global stress on ledge punching was studied in a second phase of the research using long-span beams and is presented in a separate paper.[10] Results of the experimental programs and extensive finite element modeling were used to develop simplified design guidelines for the punching-shear strength of ledges, which have been implemented in the eighth edition of the *PCI Design Handbook*.[11,12] These guidelines are intended to provide a sufficient margin of safety for the ledge capacity under a wide range of loading conditions.

Table 1. Summary of selected test parameters for 17 short-span beams

Parameter	Test location: Midspan	Test location: End	Notes
Load eccentricity e'	✓	✓	Not considered by PCI procedure
Longitudinal reinforcement in ledge	✓	✓	
Transverse reinforcement (C bars)	✓	✓	
Bearing length l_b	✓	n.d.	
Bearing pad material	n.d.	✓	
Loading duration	n.d.	✓	
Concrete strength f_c'	✓	✓	Considered by PCI procedure
Bearing width b_t	✓	✓	
Ledge height h_l	✓	✓	
Ledge projection l_p	✓	✓	
Edge distance d_e	n/a	✓	

Note: n/a = not applicable; n.d. = no data.

Experimental program

The first-phase experimental program included 21 reinforced concrete L-shaped short-span beams. Seventeen beams with standard ledge reinforcement detailing were used to study the effect of selected parameters on punching capacity, while the remaining four beams were tested to investigate the performance of special reinforcement details. The span of all tested beams was 15.5 ft (4.72 m). The geometry of the beams was typical of L-shaped beams currently used by the precast concrete industry, and the beams were designed to force ledge failure by overreinforcing other potential failure modes. All tested beams had web dimensions of 8 × 60 in. (200 × 1500 mm) (**Fig. 2**). Most of the beams had an 8 × 8 in. continuous ledge along the bottom of the inner face of the web, except for a few selected beams where the size of the ledge was varied to investigate this parameter. The ledge of each beam was cut back 12 in. (300 mm) from each end to replicate a typical field connection detail that allows the beam to be bolted to supporting columns. Two holes through the web thickness were provided at each end of all beams to facilitate bolting to the test frame with high-strength threaded rods, similar to field conditions. For each beam, the ledge was tested first under a point load at midspan, and then retested twice, once at each end. Thus, three tests were performed on each beam.

Test parameters

Table 1 lists the 11 parameters that were examined in the experimental program using 17 of the 21 short-span beams. Seven of the parameters were investigated at both midspan and end locations; four parameters were examined only at either a midspan or an end location. Five of the parameters are considered by the PCI procedure, while six others are not. Six of these seventeen beams were duplicates that were tested to provide more confidence in the test results and observations.

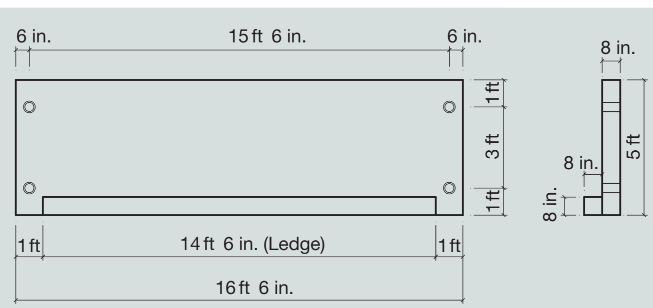

Figure 2. Typical configuration for test beams. Note: 1 in. = 25.4 mm; 1 ft = 0.305 m.

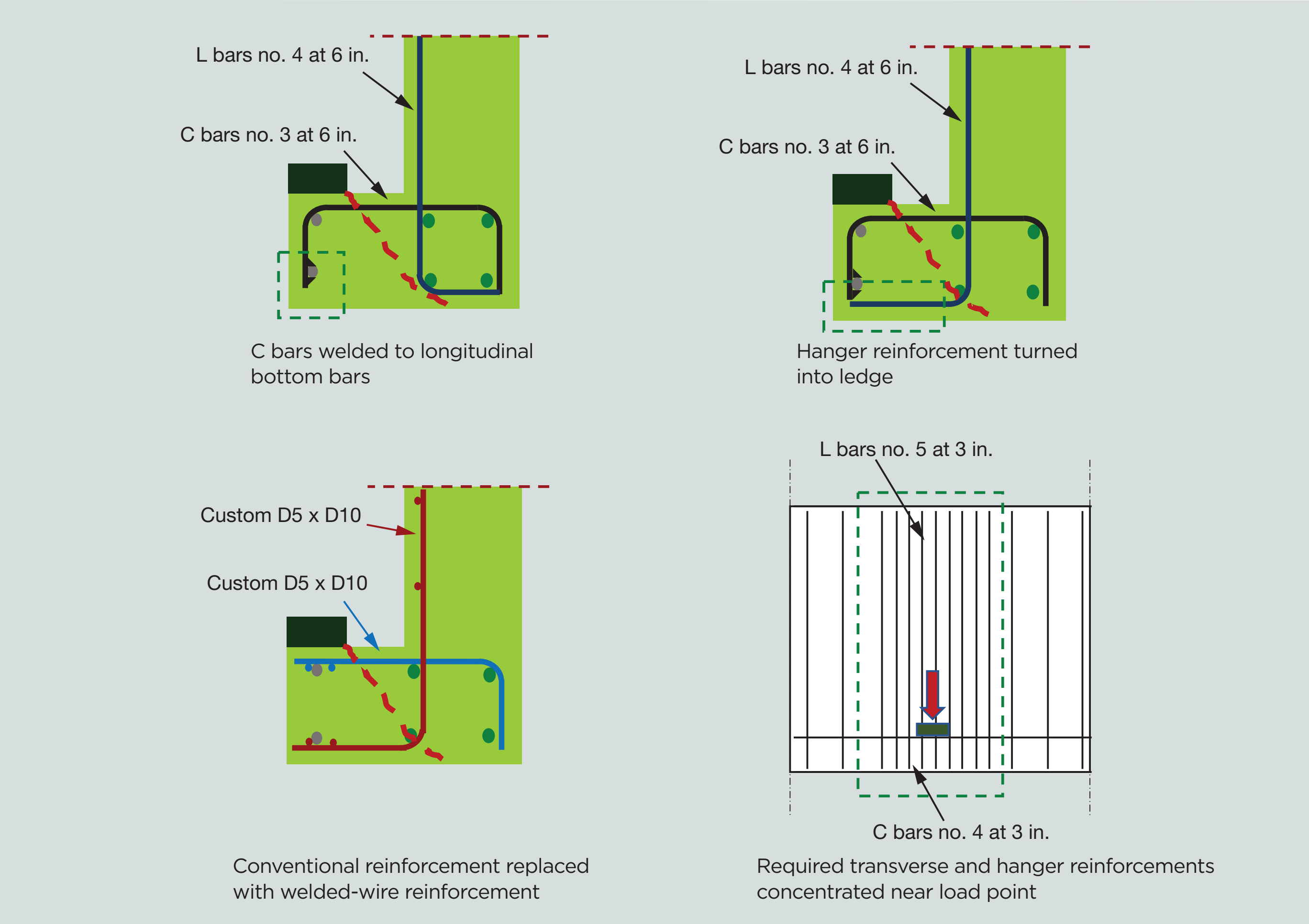

Figure 3. Special reinforcement details. Note: no. 3 = 10M; no. 4 = 13M; no. 5 = 16M; D5 = 6.4 mm; D10 = 9 mm; 1 in. = 25.4 mm.

Four of the twenty-one short-span beams were tested to investigate the performance of different special reinforcement details. The first beam, EX-RS1, included transverse reinforcement (C bars) that was welded to the longitudinal bottom bar in the ledge to examine possible enhancement of the anchorage (**Fig. 3**). The second beam, EX-RS2, included turning the hanger reinforcement (L bars) into the ledge to intercept the critical punching-shear crack (Fig. 3). In the third beam, EX-RS3, the conventional transverse and hanger reinforcement was replaced by custom-made welded-wire reinforcement (Fig. 3). Finally, the fourth beam, EX-RS4, was used to determine the effect of concentrating the required transverse and hanger reinforcement near the load point (Fig. 3). **Tables 2** and **3** summarize the details of 21 tests at midspan locations and 42 tests at end locations, respectively.

Test setup and instrumentation

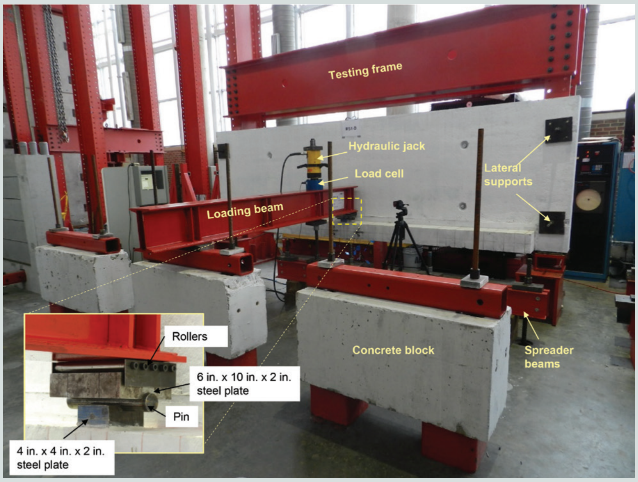

Figure 4. Test setup. Note: 1 in. = 25.4 mm.

Figure 4 shows an overall view of the test setup used for the short-span beams. All beams were supported vertically at both ends by steel stands, which were fit tightly against test frame columns post-tensioned to the floor. To maintain torsional equilibrium, the beams were tied laterally at each end to the test frame columns using two threaded rods passing through holes in the beam web. For all tests, load was applied to the ledge using a steel beam spanning between the ledge at one end and a system of supporting concrete blocks at the other end. A hydraulic jack was used to apply load to the steel beam, and the applied load was monitored by a load cell. The load was transferred to the ledge through a system of rollers to allow horizontal movement of the steel beam to minimize the

Table 2. Midspan tests for short-span beams

Specimen	Test	f'_c, psi	h_l, in.	l_p, in.	Transverse reinforcement C bars	Longitudinal reinforcement in ledge	Hanger reinforcement L bars	e', in.	l_b, in.	b_t, in.	Special reinforcement detail
RS1	RS1-M	7000	8	8	No. 3 at 6 in.	2 no. 4	No. 4 at 6 in.	6	4	4	None
RS1-D	RS1-D-M										
RS2	RS2-M	5000*			No. 3 at 7 in.		No. 4 at 7 in.			12*	
RS3	RS3-M	10,000*			No. 3 at 5 in.		No. 4 at 5 in.			4	
RS3-D	RS3-D-M										
RS4	RS4-M	7000	12*		No. 4 at 8 in.	2 no. 5	No. 4 at 4 in.				
RS5	RS5-M		10*		No. 3 at 5 in.		No. 4 at 5 in.				
RS5-D	RS5-D-M							4.5*			
RS6	RS6-M		10	6*	No. 3 at 7 in.	2 no. 4	No. 4 at 7 in.	6			
RS7	RS7-M			10*	No. 4 at 8 in.	2 no. 5	No. 4 at 4 in.				
RS7-D	RS7-D-M								8*		
RS8	RS8-M		8	8	No. 5 at 6 in.*	2 no. 4	No. 4 at 6 in.		4		
RS9	RS9-M				No. 4 at 6 in.*						
RS9-D	RS9-D-M									8*	
RS10	RS10-M				No. 3 at 6 in.	3 no. 6*				4	
RS11	RS11-M					2 no. 6*					
RS11-D	RS11-D-M										
EX-RS1	EX-RS1-M	7000	8	8	No. 3 at 6 in.	2 no. 4	No. 4 at 6 in.	6	4	4	C bars welded to longitudinal bottom bar in ledge*
EX-RS2	EX-RS2-M										Hanger reinforcement turned into ledge*
EX-RS3	EX-RS3-M				Custom D5×D10		Custom D5×D10				Welded-wire reinforcement*
EX-RS4	EX-RS4-M				No. 4 at 3 in.		No. 5 at 3 in.				Transverse/hanger reinforcement concentrated near load*

Note: e' = eccentricity of ledge vertical load to the inner web face; f'_c = specified compressive strength of concrete; h_l = height of beam ledge; l_b = bearing length; l_p = projection of the ledge. No. 3 = 10M; no. 4 = 13M; no. 5 = 16M; no. 6 = 19M; D5 = 6.4 mm; D10 = 9 mm. 1 in. = 25.4 mm; 1 psi = 6.895 kPa.

* Investigated parameter for each test

Table 3. End tests for short-span beams

<table>
<tr><th>Specimen</th><th>Test</th><th>f'_c, psi</th><th>h_l, in.</th><th>l_p, in.</th><th>Transverse reinforcement C bars</th><th>Longitudinal reinforcement in ledge</th><th>Hanger reinforcement L bars</th><th>d_e, in.</th><th>e', in</th><th>b_t, in.</th><th>Special reinforcement detail</th></tr>
<tr><td rowspan="2">RS1†,**</td><td>RS1-E1</td><td rowspan="4">7000</td><td rowspan="10">8</td><td rowspan="16">8</td><td rowspan="4">No. 3 at 6 in.</td><td rowspan="10">2 no. 4</td><td rowspan="4">No. 4 at 6 in.</td><td>16</td><td rowspan="13">6</td><td rowspan="25">4</td><td rowspan="34">None</td></tr>
<tr><td>RS1-E2</td><td>24*</td></tr>
<tr><td rowspan="2">RS1-D†,**</td><td>RS1-D-E1</td><td>16</td></tr>
<tr><td>RS1-D-E2</td><td>8*</td></tr>
<tr><td rowspan="2">RS2†,**</td><td>RS2-E1</td><td rowspan="2">5000*</td><td rowspan="2">No. 3 at 7 in.</td><td rowspan="2">No. 4 at 7 in.</td><td>16</td></tr>
<tr><td>RS2-E2</td><td>20*</td></tr>
<tr><td rowspan="2">RS3†,**</td><td>RS3-E1</td><td rowspan="4">10,000*</td><td rowspan="4">No. 3 at 5 in.</td><td rowspan="4">No. 4 at 5 in.</td><td>16</td></tr>
<tr><td>RS3-E2</td><td>24*</td></tr>
<tr><td rowspan="2">RS3-D†,**</td><td>RS3-D-E1</td><td>16</td></tr>
<tr><td>RS3-D-E2</td><td>8*</td></tr>
<tr><td rowspan="2">RS4†,**</td><td>RS4-E1</td><td rowspan="24">7000</td><td rowspan="2">12*</td><td rowspan="2">No. 4 at 8 in.</td><td rowspan="6">2 no. 5</td><td rowspan="2">No. 4 at 4 in.</td><td>16</td></tr>
<tr><td>RS4-E2</td><td>24*</td></tr>
<tr><td rowspan="2">RS5†,**</td><td>RS5-E1</td><td rowspan="4">10*</td><td rowspan="4">No. 3 at 5 in.</td><td rowspan="4">No. 4 at 5 in.</td><td rowspan="22">16</td></tr>
<tr><td>RS5-E2</td><td>4.5*</td></tr>
<tr><td rowspan="2">RS5-D†,**</td><td>RS5-D-E1</td><td>6</td></tr>
<tr><td>RS5-D-E2</td><td>3*</td></tr>
<tr><td rowspan="2">RS6†,**</td><td>RS6-E1</td><td rowspan="6">10</td><td rowspan="2">6*</td><td rowspan="2">No. 3 at 7 in.</td><td rowspan="2">2 no. 4</td><td rowspan="2">No. 4 at 7 in.</td><td>4.0*</td></tr>
<tr><td>RS6-E2</td><td>3.0*</td></tr>
<tr><td rowspan="2">RS7†,**</td><td>RS7-E1</td><td rowspan="4">10*</td><td rowspan="4">No. 4 at 8 in.</td><td rowspan="4">2 no. 5</td><td rowspan="4">No. 4 at 4 in.</td><td>6</td></tr>
<tr><td>RS7-E2</td><td>4.5*</td></tr>
<tr><td rowspan="2">RS7-D†,**</td><td>RS7-D-E1</td><td>7.5*</td></tr>
<tr><td>RS7-D-E2</td><td>3.0*</td></tr>
<tr><td rowspan="2">RS8**</td><td>RS8-E1†</td><td rowspan="12">8</td><td rowspan="12">8</td><td rowspan="2">No. 5 at 6 in.*</td><td rowspan="6">2 no. 4</td><td rowspan="12">No. 4 at 6 in.</td><td rowspan="12">6</td></tr>
<tr><td>RS8-E2‡</td></tr>
<tr><td rowspan="2">RS9†,**</td><td>RS9-E1</td><td rowspan="4">No. 4 at 6 in.*</td></tr>
<tr><td>RS9-E2</td><td>8*</td></tr>
<tr><td rowspan="2">RS9-D†,**</td><td>RS9-D-E1</td><td>4</td></tr>
<tr><td>RS9-D-E2</td><td>12*</td></tr>
<tr><td rowspan="2">RS10†</td><td>RS10-E1**</td><td rowspan="6">No. 3 at 6 in.</td><td rowspan="2">3 no. 6*</td><td rowspan="3">4</td></tr>
<tr><td>RS10-E2††</td></tr>
<tr><td rowspan="2">RS11†,**</td><td>RS11-E1</td><td rowspan="4">2 no. 6*</td></tr>
<tr><td>RS11-E2</td><td>8*</td></tr>
<tr><td rowspan="2">RS11-D†,**</td><td>RS11-D-E1</td><td>4</td></tr>
<tr><td>RS11-D-E2</td><td>12*</td></tr>
</table>

<table>
<caption>**Table 3.** End tests for short-span beams (cont.)</caption>
<tr><th>Specimen</th><th>Test</th><th>f'_c, psi</th><th>h_l, in.</th><th>l_p, in.</th><th>Transverse reinforcement C bars</th><th>Longitudinal reinforcement in ledge</th><th>Hanger reinforcement L bars</th><th>d_e, in.</th><th>e', in.</th><th>b_t, in.</th><th>Special reinforcement detail</th></tr>
<tr><td rowspan="2">EX-RS1†,**</td><td>EX-RS1-E1</td><td rowspan="8">7000</td><td rowspan="8">8</td><td rowspan="8">8</td><td rowspan="4">No. 3 at 6 in.</td><td rowspan="8">2 no. 4</td><td rowspan="4">No. 4 at 6 in.</td><td rowspan="8">16</td><td rowspan="8">6</td><td rowspan="8">4</td><td rowspan="2">C bars welded to longitudinal bottom bar in ledge*</td></tr>
<tr><td>EX-RS1-E2</td></tr>
<tr><td rowspan="2">EX-RS2†,**</td><td>EX-RS2-E1</td><td rowspan="2">Hanger reinforcement turned into ledge*</td></tr>
<tr><td>EX-RS2-E2</td></tr>
<tr><td rowspan="2">EX-RS3†,**</td><td>EX-RS3-E1</td><td rowspan="2">Custom D5xD10</td><td rowspan="2">Custom D5xD10</td><td rowspan="2">Welded-wire reinforcement*</td></tr>
<tr><td>EX-RS3-E2</td></tr>
<tr><td rowspan="2">EX-RS4†,**</td><td>EX-RS4-E1</td><td>No. 4 at 4.5 in.</td><td>No. 5 at 4.5 in.</td><td rowspan="2">Transverse/hanger reinforcement concentrated near load*</td></tr>
<tr><td>EX-RS4-E2</td><td>No. 4 at 3 in.</td><td>No. 5 at 3 in.</td></tr>
</table>

Note: d_e = distance from center of an applied concentrated load to end of ledge; e' = eccentricity of ledge vertical load to the inner web face; f'_c = specified compressive strength of concrete; h_l = height of beam ledge; l_p = projection of the ledge. No. 3 = 10M; no. 4 = 13M; no. 5 = 16M; no. 6 = 19M; D5 = 6.4 mm; D10 = 9 mm; 1 in. = 25.4 mm; 1 psi = 6.895 kPa.

* Investigated parameter for each test.

† Steel bearing pad material.

‡ Typical randomly oriented fiber pad, investigated parameter for test.

** Monotonic loading duration.

†† Sustained loading duration, investigated parameter for test.

effect of friction. A pin was also used to allow rotation of the steel beam and to ensure uniform load distribution under the bearing plate (Fig. 4). Typically, the first test was conducted at midspan to obtain an initial ledge failure. The loading system was then moved to one end to obtain a second failure and, last, to the opposite end to get a third failure out of the same beam.

Various instruments connected to an electronic data acquisition system were used to monitor each test. Cracks were marked at incremental loading steps, and photographs and videos were taken. At each test location, string potentiometers were used to monitor the vertical deflection of the ledge and the web. Two additional string potentiometers were used to monitor the lateral displacements at the top and bottom of the web. Reusable surface-mounted strain gauges, referred to as pi gauges (**Fig. 5**), were used to monitor concrete surface strains at selected locations. The gauges were applied in orthogonal pairs on the front face of the ledge on one side of the bearing plate to capture the strains resulting from the punching-shear cracks. For end tests, pi gauges were used to monitor shear strains at the end region, while for midspan tests, pi gauges were used at the top and bottom of the beam to monitor the flexural strains in the beam.

Test results

Tables 4 and **5** give the measured concrete strengths, measured ledge capacities, and ledge capacities predicted by the PCI procedure used in the seventh edition of *PCI Design Handbook*[1] for all midspan and end tests, respectively. Punching-shear failure of the ledge was observed for all tests. For the midspan tests, the results indicated that the measured ledge capacities could be as low as 72% of the values predicted by the PCI procedure. For the tests performed at end locations, the measured ledge capacity exceeded the capacity predicted by the PCI procedure for most cases; however, in some cases it could be as low as 87% of the predicted values, particularly where the edge distance of the load was relatively large. It can be concluded that even in the absence of significant global stress, the PCI procedure can overestimate ledge capacity. The overestimation appears to be more pronounced at midspan locations than at end locations.

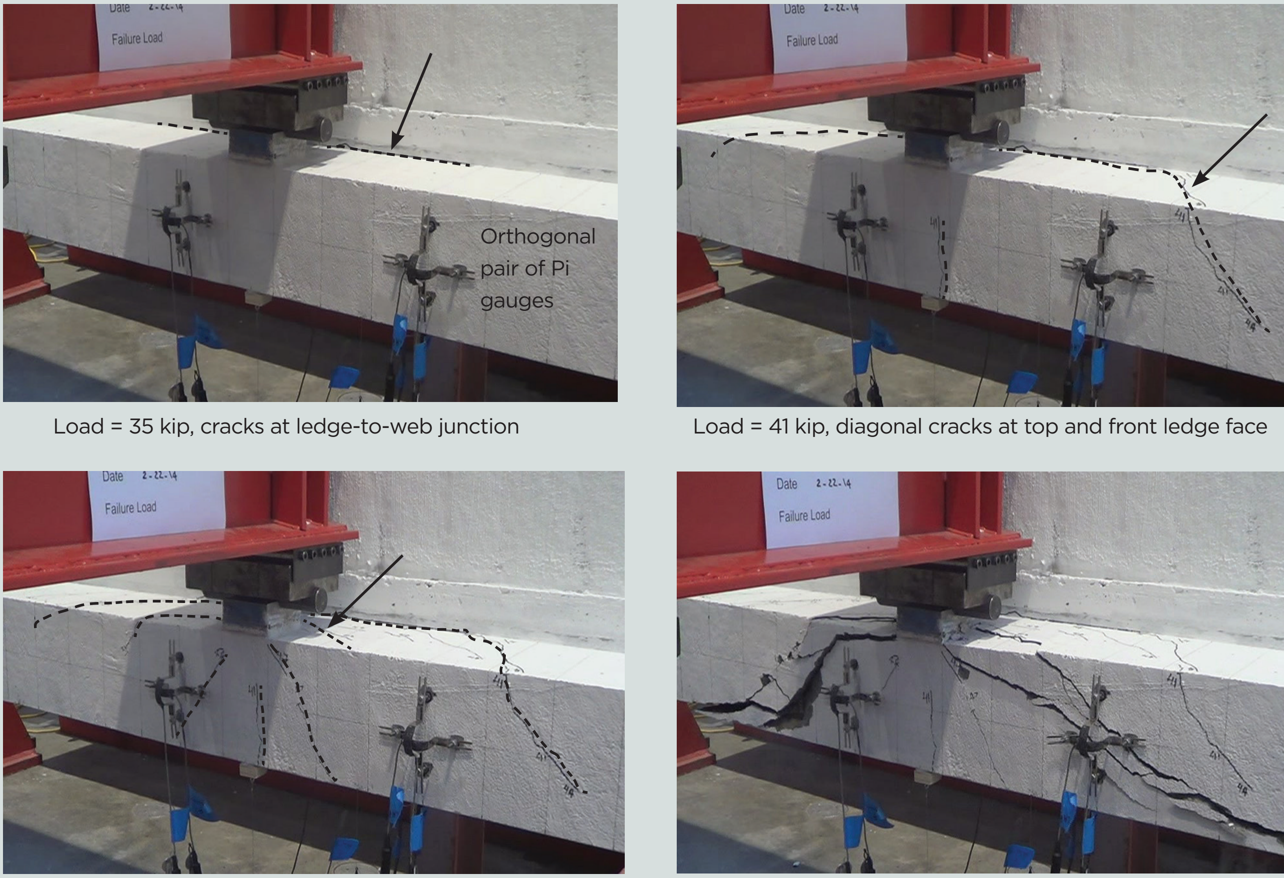

Load = 35 kip, cracks at ledge-to-web junction

Load = 41 kip, diagonal cracks at top and front ledge face

Load = 47 kip, diagonal cracks from back of bearing plate

Load = 50.6 kip, failure occurred

Figure 5. Crack pattern at different load levels up to failure, test RS3-M. Note: 1 kip = 4.448 kN.

Ledge behavior

Typical behaviors observed at midspan (Table 4, tests RS3-M and RS3-D-M) and at the end (Table 5, tests RS3-E1 and RS3-D-E1) are illustrated using beams RS3 and RS3-D. The two beams had the same concrete compressive strength of 8800 psi (61 MPa) at the time of testing and the same 8 × 8 in. (200 × 200 mm) ledge geometry. The bearing plate of 4 × 4 in. (100 × 100 mm) and the load eccentricity of 6 in. (150 mm) with respect to the inner web face were also the same for both beams.

Ledge behavior at midspan

Figure 5 shows the crack pattern of the ledge at different load levels up to failure for the midspan test RS3-M. The first crack occurred at a load level of 35 kip (155 kN) and was observed at the ledge-to-web junction. At a load level of 41 kip (180 kN), the cracks extended along the length of the ledge and propagated horizontally on the top face of the ledge with an angle toward the front face of the ledge. Prior to failure, at a load of 47 kip (210 kN), additional cracks were observed at the back of the bearing plate and extended diagonally on the horizontal surface of the ledge. Failure occurred suddenly at a load level of 50.6 kip (225 kN), with diagonal tension cracks propagating from the back and the sides of the bearing plate into the front face of the ledge.

The test was duplicated using beam RS3-D, which had the same characteristics as beam RS3. The observed ledge behavior in the duplicated test was similar to that observed in the original test. The failure load in the duplicated test was 53.2 kip (237 kN), which was 5% higher than in test RS3-M. The load-deflection diagrams for both tests indicate similar behaviors up to failure (**Fig. 6**). The concrete strains measured at the front face of the ledge increased suddenly as the diagonal tension cracks occurred at failure, while the concrete strain at the bottom of the web at midspan demonstrated low global flexural stress.

Ledge behavior at end

Tests were also conducted 16 in. (410 mm) from the end of the ledge for the two identical beams, RS3 and RS3-D. The behavior and crack pattern for the end tests were similar to those observed for the midspan tests. For test RS3-E1, the first crack initiated at a load level of 35 kip (155 kN) at the ledge-to-web junction. When the load reached 43 kip (190 kN), diagonal cracks propagated on the top face of the ledge toward the front face of the ledge.

Table 4. Midspan test results of short-span beams

Specimen	Test	Investigated parameter	Measured concrete strength f'_c, psi	Measured ledge capacity $V_{ln,Measured}$, kip	PCI ledge capacity $V_{ln,PCI}$, kip	$V_{ln,Measured}$/$V_{ln,PCI}$
RS1	RS1-M	Control	7310	47.4	57.5	0.82
RS1-D	RS1-D-M			47.3*	57.5*	0.82*
RS2	RS2-M	Bearing width b_t = 12 in.	7010	52.8	72.3	0.73
RS3	RS3-M	Concrete strength f'_c = 8800 psi	8800	50.6	63.0	0.80
RS3-D	RS3-D-M			53.2*	63.0*	0.84*
RS4	RS4-M	Ledge height h_l = 12 in.	7310	90.5	98.5	0.92
RS5	RS5-M	Ledge height h_l = 10 in.	7890	72.7	79.9	0.91
RS5-D	RS5-D-M	Load eccentricity e' = 4.5 in.		81.3	79.9	1.02
RS6	RS6-M	Ledge projection l_p = 6 in.	8640	71.9	72.5	0.99
RS7	RS7-M	Ledge projection l_p = 10 in.		80.1	94.8	0.84
RS7-D	RS7-D-M	Bearing length l_b = 8 in.		77.6	94.8	0.82
RS8	RS8-M	Transverse reinforcement no. 5 at 6 in.		54.7	62.5	0.88
RS9	RS9-M	Transverse reinforcement no. 4 at 6 in.	7730	46.4	59.1	0.79
RS9-D	RS9-D-M	Bearing width b_t = 8 in.		51.1	67.5	0.76
RS10	RS10-M	Longitudinal reinforcement 3 no. 6		52.5	59.1	0.89
RS11	RS11-M	Longitudinal reinforcement 2 no. 6	7910	50.1	59.8	0.84
RS11-D	RS11-D-M		7730	46.0*	59.1*	0.78*
EX-RS1	EX-RS1-M	Special reinforcement detail C bars welded to longitudinal bottom bar in ledge	10,530	49.4	69.0	0.72
EX-RS2	EX-RS2-M	Special reinforcement detail hanger reinforcement turned into ledge		61.1	69.0	0.89
EX-RS3	EX-RS3-M	Special reinforcement detail welded-wire reinforcement		53.4	69.0	0.77
EX-RS4	EX-RS4-M	Special reinforcement detail transverse/hanger reinforcement concentrated near load		77.0	69.0	1.12

Note: no. 4 = 13M; no. 5 = 16M; no. 6 = 19M; 1 in. = 25.4 mm; 1 kip = 4.448 kN; 1 psi = 6.895 kPa.

* Duplicate test to test in previous row

Table 5. End test results of short-span beams

Specimen	Test	Investigated parameter	Measured concrete strength f'_c, psi	Measured ledge capacity $V_{ln,Measured}$, kip	PCI ledge capacity $V_{ln,PCI}$, kip	$V_{ln,Measured}$/ $V_{ln,PCI}$
RS1	RS1-E1	Control	7310	42.2	41.0	1.03
	RS1-E2	Edge distance d_e = 24 in.		45.4	52.0	0.87
RS1-D	RS1-D-E1	Control		45.0*	41.0*	1.10*
	RS1-D-E2	Edge distance d_e = 8 in.		31.2	30.1	1.04
RS2	RS2-E1	Concrete strength f'_c = 7010 psi	7010	45.1	40.2	1.12
	RS2-E2	Edge distance d_e = 20 in.		42.9	45.5	0.94
RS3	RS3-E1	Concrete strength f'_c = 8800 psi	8800	47.5	45.0	1.05
	RS3-E2	Edge distance d_e = 24 in.		50.1	57.0	0.88
RS3-D	RS3-D-E1	Concrete strength f'_c = 8800 psi		45.3*	45.0*	1.01*
	RS3-D-E2	Edge distance d_e = 8 in.		38.5	33.0	1.17
RS4	RS4-E1	Ledge height h_l = 12 in.	7310	74.8	65.7	1.14
	RS4-E2	Edge distance d_e = 24 in.		84.6	82.1	1.03
RS5	RS5-E1	Ledge height h_l = 10 in.	7890	67.7	55.1	1.23
	RS5-E2	Load eccentricity e' = 4.5 in.		87.4	55.1	1.59
RS5-D	RS5-D-E1	Ledge height h_l = 10 in.		66.5*	55.1*	1.21*
	RS5-D-E2	Load eccentricity e' = 3 in.		95.7	55.1	1.74
RS6	RS6-E1	Ledge projection l_p = 6 in.	8640	71.8	53.9	1.33
	RS6-E2	Load eccentricity e' = 3 in.		78.7	53.9	1.46
RS7	RS7-E1	Ledge projection l_p = 10 in.		63.6	61.3	1.04
	RS7-E2	Load eccentricity e' = 4.5 in.		75.5	61.3	1.23
RS7-D	RS7-D-E1	Load eccentricity e' = 7.5 in.		60.3	61.3	0.98
	RS7-D-E2	Load eccentricity e' = 3 in.		94.4	61.3	1.54
RS8	RS8-E1	Transverse reinforcement no. 5 at 6 in.		49.8	44.6	1.12
	RS8-E2	Bearing pad material (typical randomly oriented fiber pad)		49.4	44.6	1.11
RS9	RS9-E1	Transverse reinforcement no. 4 at 6 in.	7730	40.3	42.2	0.95
	RS9-E2	Bearing width b_t = 8 in.		52.4	45.0	1.16
RS9-D	RS9-D-E1	Transverse reinforcement no. 4 at 6 in.		46.5*	42.2*	1.10*
	RS9-D-E2	Bearing width b_t = 12 in.		51.6	47.8	1.08
RS10	RS10-E1	Longitudinal reinforcement 3 no. 6		45.6	42.2	1.08
	RS10-E2	Loading duration (sustained load)		48.0	42.2	1.14
RS11	RS11-E1	Longitudinal reinforcement 2 no. 6	7910	43.5	42.7	1.02
	RS11-E2	Bearing width b_t = 8 in.		50.2	45.5	1.10

Table 5. End test results of short-span beams (cont.)

Specimen	Test	Investigated parameter	Measured concrete strength f'_c, psi	Measured ledge capacity $V_{ln,Measured}$, kip	PCI ledge capacity $V_{ln,PCI}$, kip	$V_{ln,Measured}$/ $V_{ln,PCI}$
RS11-D	RS11-D-E1	Longitudinal reinforcement 2 no. 6	7730	42.5*	42.2*	1.01*
	RS11-D-E2	Bearing width b_t = 12 in.		48.5	47.8	1.01
EX-RS1	EX-RS1-E1	Special reinforcement detail C bars welded to longitudinal bottom bar in ledge	10,530	52.0	49.3	1.06
	EX-RS1-E2			52.0†	49.3†	1.06†
EX-RS2	EX-RS2-E1	Special reinforcement detail hanger reinforcement turned into ledge		53.3	49.3	1.08
	EX-RS2-E2			54.8†	49.3†	1.11†
EX-RS3	EX-RS3-E1	Special reinforcement detail welded-wire reinforcement		53.1	49.3	1.08
	EX-RS3-E2			53.1†	49.3†	1.08†
EX-RS4	EX-RS4-E1	Special reinforcement detail transverse/ hanger reinforcement concentrated near load (C bars no. 4 at 4.5 in., L bars no. 5 at 4.5 in.)		75.2	49.3	1.53
	EX-RS4-E2	Special reinforcement detail transverse/ hanger reinforcement concentrated near load (C bars no. 4 at 3.0 in., L bars no. 5 at 3.0 in.)		86.5	49.3	1.76

Note: No. 4 = 13M; no. 5 = 16M; no. 6 = 19M; 1 in. = 25.4 mm; 1 kip = 4.448 kN; 1 psi = 6.895 kPa.

* Duplicate test to test in two rows above

† Duplicate test to test in previous row

Prior to failure, at a load level of 46 kip (205 kN), a crack initiated from the back of the bearing plate with an angle of 27 degrees toward the front face of the ledge. The crack continued to propagate on the front face of the ledge from one side; however, the crack extended from the other side along the length of the beam until it reached the end of the ledge. The crack then extended on the side of the ledge until it reached the web. Failure occurred suddenly at a load level of 47.5 kip (211 kN), accompanied by diagonal tension cracks propagating from the back of the bearing plate on one side into the front face of the ledge and on the other side into the top face of the ledge toward the end of the ledge. No shear cracks were observed on the inner face of the web because the applied global shear stress was quite low.

The test was duplicated at one end for the identical beam, RS3-D. The crack pattern up to failure in the duplicated test was similar to that observed in the original test. The failure load was 45.3 kip (201 kN), which was 5% less than the measured failure load of test RS3-E1. The load-deflection diagrams for both tests indicated similar ledge behavior up to failure.

Configuration of failure surface

Figures 7 and **8** show the observed failure surfaces for midspan test RS3-M and end test RS3-E1, respectively. A typical failure surface is formed initially by cracks developing at the back of the bearing plate and extending on the top face of the ledge on both sides at an average angle of 27 degrees with respect to web face (Fig. 7). The cracks then extend into the front face of the ledge with an average angle of 34 degrees with respect to the horizontal. The angles and the overall size

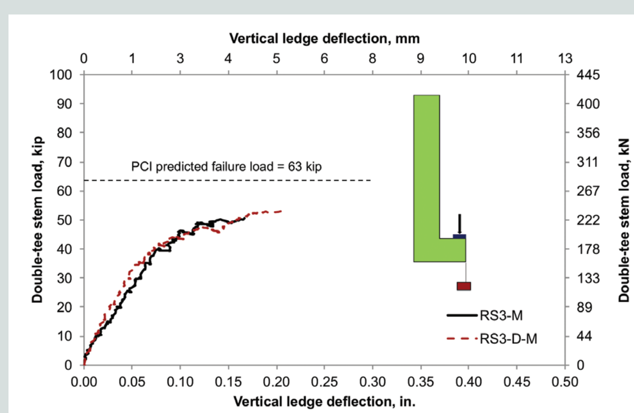

Figure 6. Measured ledge vertical deflections at midspan for tests RS3-M and RS3-D-M. Note: 1 kip = 4.448 kN.

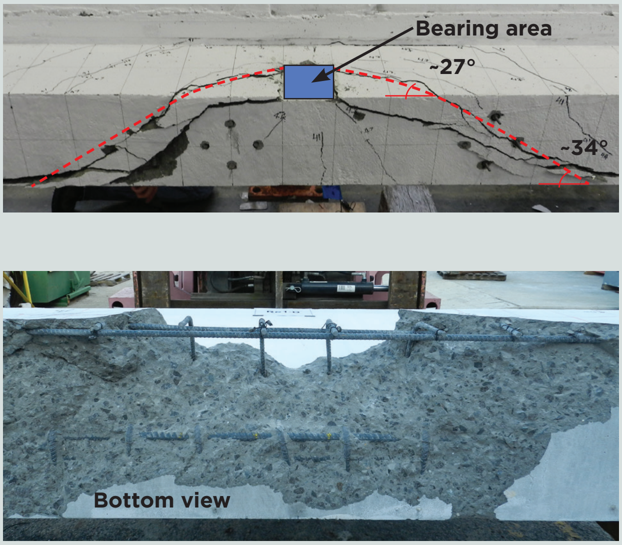

Figure 7. Observed failure surface at midspan, test RS3-M.

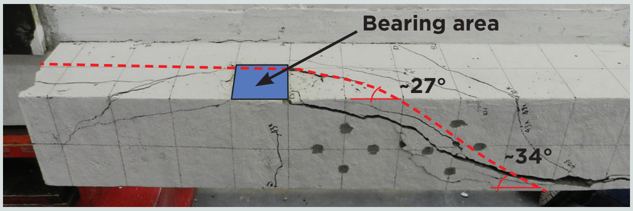

Figure 8. Observed failure surface at end, test RS3-E1.

of the failure surface are influenced by several parameters, such as load eccentricity, ledge height, and concentration of ledge reinforcement, which are discussed in the following sections. After chipping away the cracked concrete postfailure, the bottom view of a typical failure surface revealed that the crack extended into the bottom of the beam and bypassed the hanger bars (Fig. 7). If the applied load was sufficiently close to the end of the ledge, the failure surface would be asymmetric (Fig. 8). While the PCI procedure assumes 45-degree failure planes developing from the sides of the bearing pads, the observed failure planes were generally inclined at a shallower angle, resulting in a larger failure surface. The PCI procedure can overestimate the ledge capacity under a variety of conditions. This overestimation can be primarily attributed to the effects of global stress interacting with localized ledge shear stress, a parameter not considered by PCI procedure.

Effect of various parameters

Due to the variation of concrete strengths among the tested specimens, the results are normalized to highlight the effect of each parameter independently from the effect of concrete strength. The normalization was performed by expressing the results in terms of $V_{ln}/\sqrt{f_c'}$, where V_{ln} is the measured nominal ledge capacity, whether at midspan or at the end, and f_c' is the measured concrete compressive strength at the time of testing (Tables 4 and 5). The results are not normalized when evaluating the effect of concrete strength itself. For duplicated tests, the averages of the measured ledge capacities were used to evaluate the effect of each parameter. The effects of 11 parameters, investigated through 17 short-span beams, are discussed in the following sections.

Load eccentricity

The effect of load eccentricity e' from the inner web face (Fig. 2) was investigated at the midspan test locations of beams RS5 and RS5-D, where the ledge projection was 8 in. (200 mm). The load eccentricity was increased from 4.5 in. (115 mm) for beam RS5-D to 6 in. (150 mm) for beam RS5. At end locations of the same two beams, the effect of load eccentricity was also investigated by increasing the load eccentricity from 3 to 6 in. (75 to 150 mm). The same effect was also examined at end locations of beams RS7 and RS7-D, where the ledge projection was 10 in. (250 mm) and the load eccentricity was increased from 3 in. for beam RS7 to 7.5 in. (190 mm) for beam RS7-D.

The test results (Tables 4 and 5) indicate that when the load eccentricity was increased by 33% at midspan, the ledge capacity was reduced by 10%. Similarly, when the load eccentricity at the end location was increased by 100% for beams RS5 and RS5-D and by 150% for beams RS7 and RS7-D, the ledge capacities were reduced by 30% and 36%, respectively. The reduction of ledge capacity was more pronounced at the end of the beam, where the applied global shear stress was more significant. It is concluded, therefore, that increasing the load eccentricity can significantly reduce the ledge capacity, especially at the end of a beam. Observations during the tests indicated that increasing the load eccentricity from the inner web face had little effect on the angles of the shear cracks that still propagated on the top surface of the ledge from the back edge of the bearing plate. Hence, increasing the load eccentricity from the inner web face reduced the overall size of the failure surface and thus reduced the failure load (**Fig. 9**).

Longitudinal reinforcement in ledge

The effect of longitudinal reinforcement in the ledge (Fig. 1) was investigated using three different quantities of longitudinal steel. The amount of longitudinal reinforcement was increased from two no. 4 (13M) bars for beams RS1 and RS1-D (total reinforcement area of 0.4 in.^{2} [258 mm^2]) to two no. 6 (19M) bars in beams RS11 and RS11-D (total reinforcement area of 0.88 in.^{2} [567 mm^2]). The longitudinal reinforcement was further increased to three no. 6 bars in beam RS10 (total reinforcement area of 1.32 in.^{2} [852 mm^2]), where two no. 6 bars were placed directly under the bearing plate.

Test results at midspan and at the ends (Tables 4 and 5) indicate that increasing the amount of longitudinal reinforcement in the ledge caused only a slight increase in the ledge capacity by 8% and 2%, respectively. The increase was not proportional to the increase in reinforcement ratio, and using additional reinforcement did not change the brittleness of the failure. Therefore, it is concluded that in the absence of significant global stress, increasing the longitudinal reinforcement in a ledge has minimal effect on the capacity and the behavior of the ledge.

Transverse reinforcement (C bars)

The effect of transverse reinforcement (Fig. 1) was investigated using three different levels of transverse reinforcement. In beams RS1 and RS1-D, the transverse reinforcement was no. 3 at 6 in. (10M at 150 mm) with a total reinforcement area of 0.22 in.^{2}/ft (465 mm^2/m), while the bar size was increased for beams RS9 and RS9-D to no. 4 (13M) at 6 in. with a total reinforcement area of 0.4 in.^{2}/ft (846 mm^2/m). The transverse reinforcement in beam RS8 was further increased to no. 5 (16M) at 6 in., with a total reinforcement area of 0.62 in.^{2}/ft (1312 mm^2/m).

Test results (Tables 4 and 5) show that increasing the transverse reinforcement by 181% caused the ledge capacity to increase by 6% at midspan and by 5% at the end. Observations made during the tests indicate that increasing the quantity of transverse reinforcement had no effect on the brittleness of the failure. Therefore, it is concluded that increasing the amount of transverse reinforcement can only slightly increase ledge capacity and that such an increase is not proportional to the increase in the amount of the provided transverse reinforcement.

Bearing length

The effect of the bearing length l_b on the ledge capacity was examined only at midspan by increasing the bearing length from 4 in. (100 mm) for beam RS7 to 8 in. (200 mm) for beam RS7-D (**Fig. 10**). For both cases, the load was applied in the same manner using the same eccentricity from the center of the load to the inner web face. Test results (Table 4) indicate that increasing the bearing length had a negligible effect on the ledge capacity, which may be attributed to the fact that the induced increase in the failure surface size was small due to maintaining same the loading eccentricity for each test.

Bearing pad material

The effect of bearing pad material was investigated at the end location using two different materials. At one end of beam RS8, a 2 in. (50 mm) thick steel bearing plate was used (grouted to the ledge), while at the other end of the same beam, a 0.5 in. (12.5 mm) thick typical randomly oriented fiber pad was placed underneath the steel bearing plate. Test results at the two ends (Table 5) indicate that the variation of bearing pad material had no effect on the ledge capacity.

Loading duration

The effect of load duration was investigated at an end location by using an applied monotonic load at one end of beam RS10 and a 24-hour sustained factored load for the other end of the same beam. In the latter case, the ledge was loaded initially to the service level and then subjected to cycles of unloading

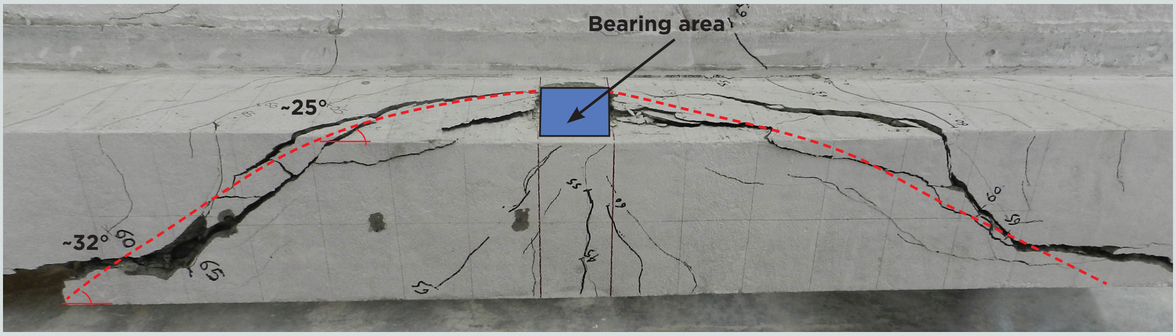

Eccentricity = 4.5 in., test RS5-D-M

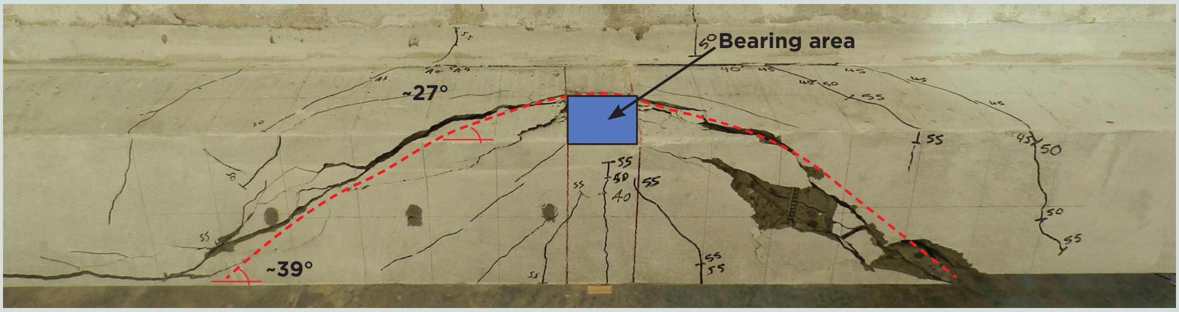

Eccentricity = 6 in., test RS5-M

Figure 9. Effect of load eccentricity on observed failure surface. Note: 1 in. = 25.4 mm.

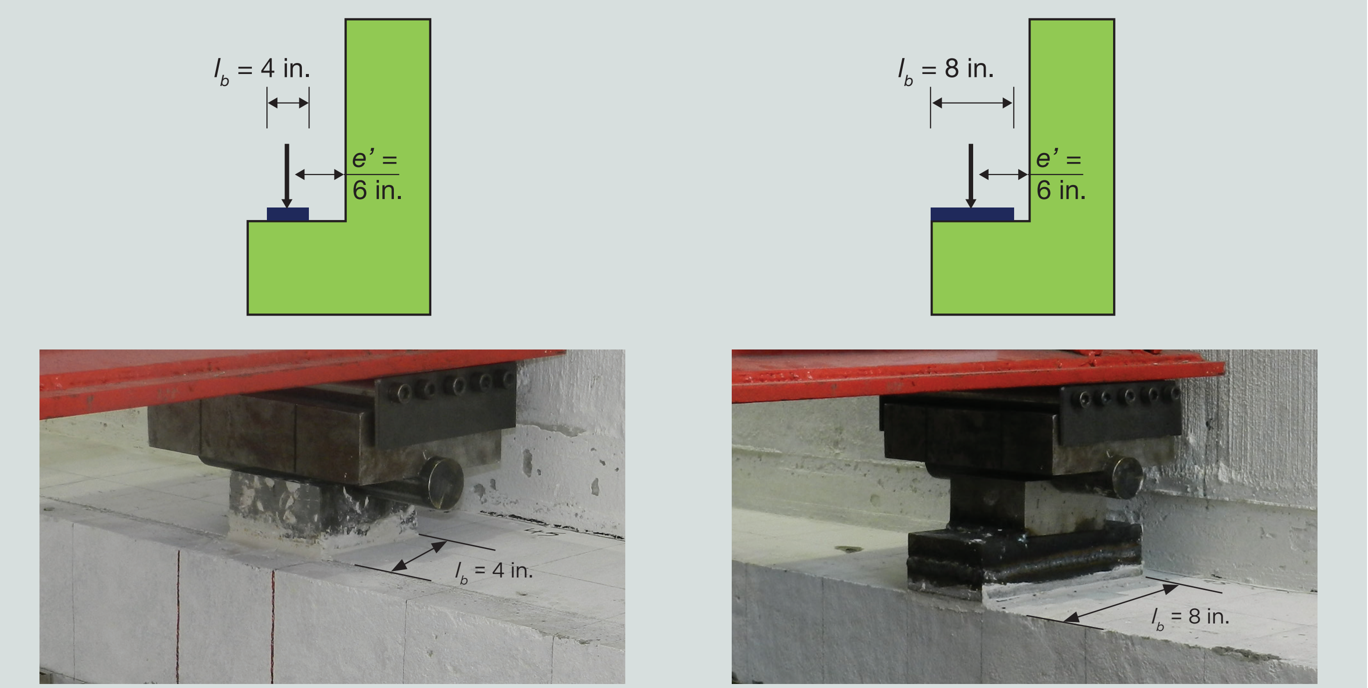

Figure 10. Different bearing lengths. Note: l_b = bearing length; e' = load eccentricity of ledge vertical load to the inner web face. 1 in. = 25.4 mm.

and reloading up to the factored load level. At the factored load stage, the load was held on the ledge for 24 hours. The ledge was then unloaded and allowed to recover for 1 hour. At the end of the recovery, the ledge was loaded again and incrementally increasing load cycles were applied to failure. The failure load of the first end test was used to estimate the service and factored load levels to use for the sustained load test at the opposite end.

Test results indicate similar ledge behavior for both tests up to failure (**Fig. 11**). However, it was observed that the diagonal cracks at the top face of the ledge occurred at 34.2 kip (152 kN) for the sustained load test compared with a load level of 40 kip (180 kN) for the monotonic loading. In terms of the crack pattern and the failure surface, no discernible difference was observed for both tests. Test results also indicate negligible effects on the ledge capacity at failure for the two loading conditions.

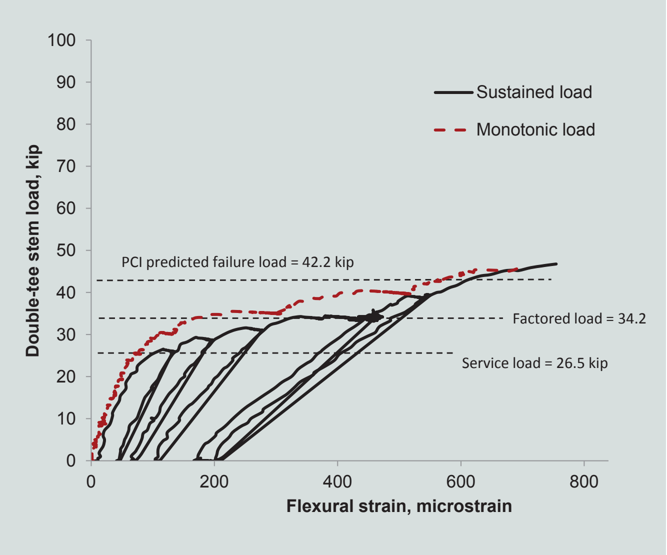

Figure 11. Effect of sustained load at end. Note: 1 kip = 4.448 kN.

Concrete strength

The effect of concrete compressive strength f_c' was investigated by comparing the test results of beams RS1 and RS1-D, which had a measured concrete strength of 7310 psi (50.4 MPa), with the test results of beams RS3 and RS3-D, which had a measured concrete strength of 8800 psi (60.7 MPa). As expected, the test results (Tables 4 and 5) indicate that increasing the concrete strength caused the ledge capacity to increase by 10% at midspan and by 6% at the end. Therefore, it is concluded that in the absence of significant global stress or prestressing, the observed increases are approximately in proportion to the 10% increase of $\sqrt{f_c'}$.

Bearing width

The effect of bearing width b_t (Fig. 1) on the ledge capacity was investigated for two load locations. At midspan, the bearing width was increased from 4 in. (100 mm) for beams RS1 and RS1-D to 8 in. (200 mm) for beam RS9-D and to 12 in. (300 mm) for beam RS2. At the ends, the bearing width was increased from 4 to 8 in. for beams RS9 and RS9-D and to 12 in. for beams RS11 and RS11-D. At end locations, the distance from the load to the ledge end was kept the same while the bearing width was increased.

There was a noticeable increase in the ledge capacity with increased bearing width for all cases due to increased failure surface area (Tables 4 and 5). When the bearing width increased from 4 to 12 in. (100 to 300 mm), the ledge capacity increased by 14% at midspan and by 19% and 13% at the beams ends. Notably, when the bearing width was increased to 12 in. (300 mm) at the ends, the ledge capacity increased only slightly over that observed for the 8 in. bearing width. This result can be attributed to the fact that the distance from the center of the load to end of the ledge was fixed at 16 in. (410 mm), regardless of the bearing width. Such distance from the end was sufficient to allow for a larger failure surface when increasing the bearing width from 4 to 8 in. However, increasing the bearing width from 8 to 12 in. allowed for no further increase in the size of the failure surface, given the 16 in. edge distance. Changing the bearing width had no effect on the angles of the failure surface.

Ledge height

The effect of ledge height h_l (Fig. 1) on the ledge capacity was investigated by increasing h_l from 8 in. (200 mm) in beams RS1 and RS1-D to 10 in. (250 mm) in beams RS5 and RS5-D and to 12 in. (300 mm) in beam RS4. The results indicate that the ledge height is the most influential parameter on the punching-shear capacity of the ledge. A 50% increase in ledge height (from 8 to 12 in.) caused the ledge capacity to increase by 91% at midspan and by 72% at the end, respectively (Tables 4 and 5). Test results also indicate that increasing the ledge height has little or no effect on the angles of the shear cracks propagating on the top face of the ledge from the back of the bearing plate. However, increasing the ledge height increased the angle of the shear cracks on the front face of the ledge (relative to horizontal) (**Fig. 12**).

Ledge projection

To examine the effect of ledge projection l_p (Fig. 1), the ledge projection at midspan was increased from 6 in. (150 mm) for beam RS6 to 8 in. (200 mm) for beam RS5 while the load was applied at $\frac{3}{4}l_p$ from the inner web face, in accordance with the PCI procedure, to achieve maximum load eccentricity. At the ends, two approaches were used to investigate the effect of ledge projection. In the first approach, the ledge projection was increased from 6 in. for beam RS6 to 8 in. for beam RS5 and to 10 in. (250 mm) for beam RS7, with the load always being applied at $\frac{3}{4}l_p$ from the web. In the second approach, the load eccentricity was fixed at 3 in. (75 mm) from the web for all three ledge projections.

Test results (Tables 4 and 5) show that increasing the ledge projection at midspan by 33%, accompanied by the associated increased load eccentricity, caused the ledge capacity to increase by only 6%. At the ends, test results indicate that with ledge projection and eccentricity both increased by 67%, ledge capacity decreased by 16%. When the same increase in ledge projection was tested at a constant load eccentricity of 3 in. (75 mm), ledge capacity increased by 20% at the end.

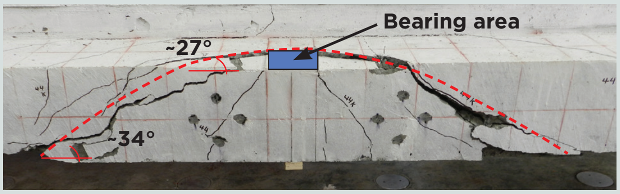

Ledge height = 8 in., test RS1-D-M

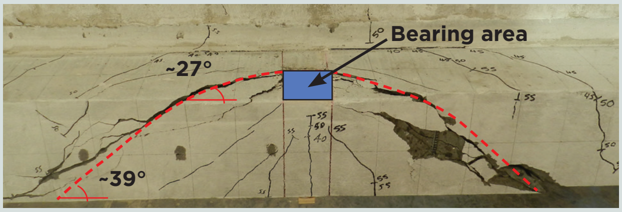

Ledge height = 10 in., test RS5-M

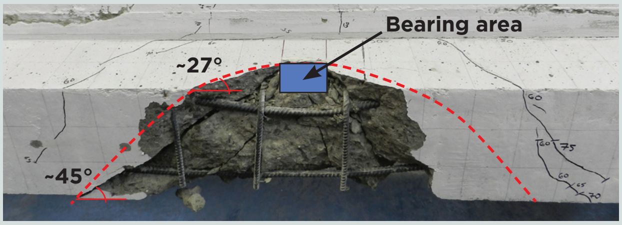

Ledge height = 12 in., test RS4-M

Figure 12. Effect of ledge height on observed failure surface. Note: 1 in. = 25.4 mm.

Edge distance

The effect of the edge distance from the load to the end of the ledge d_e (Fig. 1) on the ledge capacity was investigated using beams RS1, RS1-D, and RS2. In these tests, edge distances were increased from 8 to 16 in. (200 to 410 mm), then to 20 in. (500 mm), and then to 24 in. (610 mm). Similarly, this parameter was also investigated using beams RS3 and RS3-D, where the edge distances were increased from 8 to 16 in. and then to 24 in.

Test results indicate that increasing the edge distance generally increased the ledge capacity (Table 5). When the edge distance was increased to more than 16 in. (410 mm), the effect on the ledge capacity was negligible and the shape of the failure surface changed from an asymmetric failure to a symmetric failure (**Fig. 13**). **Table 6** summarizes the experimental results of the parametric study.

Special reinforcement details

Four different special reinforcement details were examined in this research program to determine their ability to enhance ledge capacity and to improve failure mode.

Welding C bars to longitudinal bar

Beam EX-RS1 was tested to determine the potential benefits of enhancing the anchorage for the transverse reinforcement C bars. Without using this detail, the standard C bars may not have sufficient anchorage for arresting cracks typically observed when the critical section is at the location of the applied load (Fig. 3). The C bars were welded to the longitudinal bottom bar at all locations to provide better anchorage. Using this detail would increase the fabrication time and cost and might not be practical in all plants.

Comparing the test results of beam EX-RS1 with those of beams RS1 and RS1-D (Tables 4 and 5) shows that the welded detail reduced the ledge capacity at midspan by 13% when compared on a normalized basis. The detail had a negligible effect on the ledge capacity at the end. There was no effect on the brittleness of the failure. It is concluded that welding the C bars to the longitudinal bottom bar in the ledge has a negligible effect on the capacity and does not enhance ledge behavior.

Turning hanger reinforcement into the ledge

The L-shaped hanger reinforcement in beam EX-RS2 was turned into the ledge to intercept the critical punching crack. Such a detail was expected to provide better resistance to the strut induced by the applied load by intersecting the critical crack (Fig. 3). Fabrication of this detail was found to be no more difficult than the typical arrangement of turning the hanger reinforcement into the web.

The effect of this detail was investigated by comparing the test results of beam EX-RS2 with the results of beams RS1 and RS1-D (Tables 4 and 5). Test results indicate that turning the hanger reinforcement into the ledge reduced the brittleness of the failure. The results also show that by using such a detail, ledge capacity was increased by 7% at midspan and by 3% at the end. Thus, it is concluded that turning the hanger reinforcement into the ledge has the benefit of reducing the brittleness of the failure but has a limited effect on ledge capacity.

Welded-wire reinforcement

Beam EX-RS3 was used to study the effect of using custom-deformed welded-wire reinforcement to replace traditional transverse reinforcement C bars and hanger reinforcement L bars (Fig. 3). A significant advantage of using welded-wire reinforcement is reduced fabrication time.

Comparing the results of beam EX-RS3 with those of beams RS1 and RS1-D shows that welded-wire reinforcement had virtually no effect on the brittleness of the failure, despite the fact that the hanger reinforcement was turned into the ledge. This finding can be attributed to the absence of the vertical legs common to conventional transverse reinforcement C bars, leading to a more brittle failure and offsetting the benefit of turning the hanger reinforcement into the ledge (Fig. 3). The test results indicate negligible differences in the measured ledge capacities between the two reinforcement schemes, whether at the midspan or at the end (Tables 4 and 5). Therefore, it is concluded that welded-wire reinforcement performs the same as conventional ledge reinforcement but is more advantageous in terms of time saved during fabrication.

Concentrated ledge reinforcement

Beam EX-RS4 was used to examine the effect of concentrating the required ledge reinforcement (C bars and L bars) in a group near the location of the applied loads (Fig. 3). The hanger and transverse ledge reinforcement in this beam was distributed within a 2 ft (0.6 m) zone centered at the mid-

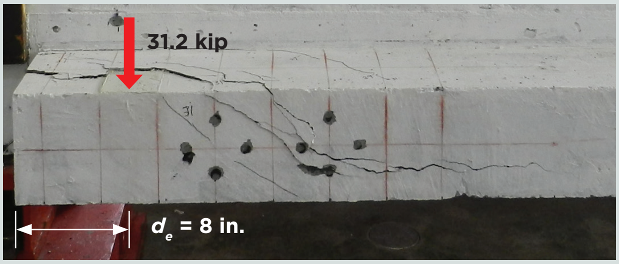

Asymmetric failure, test RS1-D-E2: d_e = 8 in., f'_c = 7310 psi

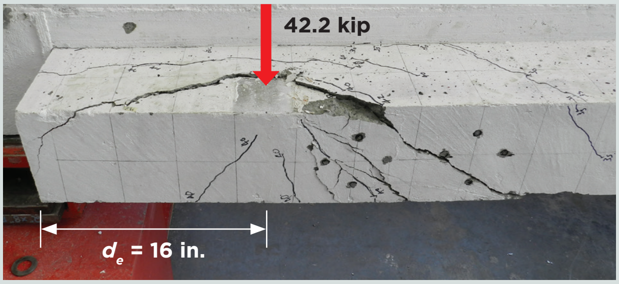

Asymmetric failure, test RS1-E1: d_e = 16 in., f'_c = 7310 psi

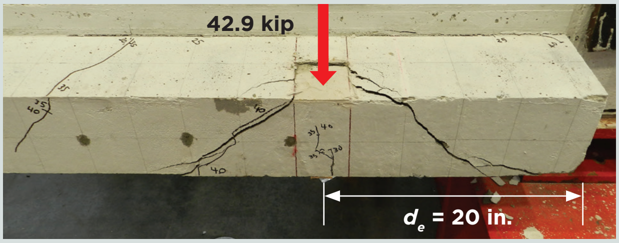

Symmetric failure, test RS2-E2: d_e = 20 in., f'_c = 7010 psi

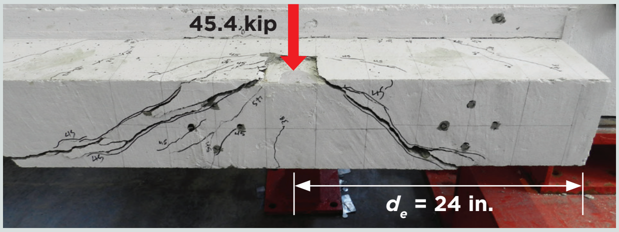

Symmetric failure, test RS1-E2: d_e = 24 in., f'_c = 7310 psi

Figure 13. Effect of edge distance on failure surface. Note: All loads are in kip. d_e = edge distance; f'_c = concrete strength. 1 in. = 25.4 mm; 1 psi = 6.895 kPa; 1 kip = 4.448 kN.

Table 6. Summary of experimental results of the parametric study

Parameter description			Increase/decrease of $V_{ln}/\sqrt{f_c'}$, %		Parameter effect on ledge capacity
			Midspan	End	
Load eccentricity e'	4.5 to 6 in. (33% increase)		-10	n.d.	Increasing load eccentricity significantly reduces ledge capacity.
	3 to 6 in. (100% increase)		n.d.	-30	
	3 to 7.5 in. (150% increase)			-36	
Longitudinal reinforcement in ledge	Two no. 4 to three no. 6 (230% increase)		+8	+2	Increasing longitudinal reinforcement or transverse steel slightly increases ledge capacity.
Transverse reinforcement (C bars)	No. 3 at 6 in. to no. 5 at 6 in. (181% increase)		+6	+5	
Bearing length l_b	4 to 8 in. (100% increase)		-3	n.d.	Bearing length, bearing pad material, or loading duration have negligible effects on ledge capacity.
Bearing pad material	Steel plate to typical randomly oriented fiber pad		n.d.	-1	
Loading duration	Monotonic to sustained load		n.d.	+5	
Concrete strength f_c'	7310 to 8800 psi (10% increase of $\sqrt{f_c'}$)		+10	+6	Increasing concrete strength significantly increases ledge capacity.
Bearing width b_t	4 to 12 in. (200% increase)		+14	+13 to 19	Increasing bearing width slightly increases ledge capacity.
Ledge height h_l	8 to 12 in. (50% increase)		+91	+72	Increasing ledge height significantly increases ledge capacity.
Ledge projection l_p	Maximum load eccentricity $e' = 0.75l_p$	6 to 8 in. (33% increase)	+6	n.d.	The effect of ledge projection depends on load eccentricity and location along the span.
		6 to 10 in. (67% increase)	n.d.	-16	
	Fixed load eccentricity e' = 3 in.	6 to 10 in. (67% increase)		+20	
Edge distance d_e	8 to 24 in. (200% increase)		n.d.	+30 to 45	Increasing edge distance significantly increases ledge capacity.

Note: n.d. = no data; V_{ln} = nominal ledge capacity. No. 3 = 10M; no. 4 = 13M; no. 5 = 16M; no. 6 = 19M; 1 in. = 25.4 mm; 1 psi = 6.895 kPa.

span load point and within 2 and 3 ft (0.6 and 0.9 m) zones centered at the end load points. The hanger reinforcement was turned into the ledge at all locations. Between these groups of concentrated reinforcement, the minimum amount of ledge reinforcement was provided as required by the PCI procedure.

The effect of concentrating the ledge reinforcement was investigated by comparing test results of beam EX-RS4 with those of beams RS1 and RS1-D, where the ledge reinforcement was distributed in a continuous fashion. Unlike the ledge failures typically observed in previous tests, the diagonal tension cracks on the top and front faces of the ledge of beam EX-RS4 did not indicate an impending failure, as the concentrated reinforcement substantially increased the failure load. Test results indicate that by concentrating the ledge reinforcement within a 2 ft (0.6 m) zone surrounding the load location, the ledge capacity at midspan was increased by 36% (Table 4). At the end location, test results also show that the ledge reinforcement concentrated near the load increased the ledge capacity by 65% (Table 5). Despite limited tests, the results suggest that concentrating the ledge reinforcement close to the load location can significantly enhance the ledge capacity. This approach can serve as a practical reinforcing alternative for heavy loading cases, in addition to other available options of increasing the ledge height or concrete strength. Test results also indicate that concentrating the ledge reinforcement within the failure zone results in steeper angles of the developing shear cracks, which consequently decreases the size of the failure surface (**Fig. 14**).

Figure 15 shows a load-deflection diagram for end tests conducted for the four reinforcement details.

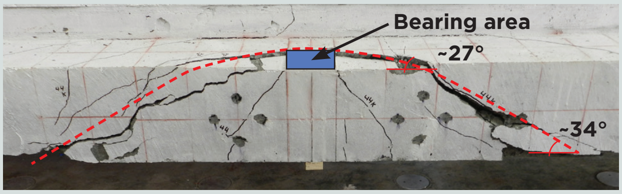

Uniform distribution of ledge reinforcement, test RS1-D-M

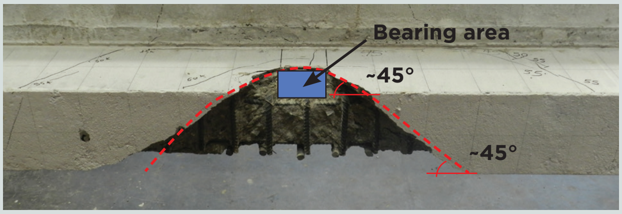

Concentrated ledge reinforcement within length of 2 ft, test EX-RS4-M

Figure 14. Effect of concentrated ledge reinforcement on observed failure surface. Note: 1 ft = 0.305 m.

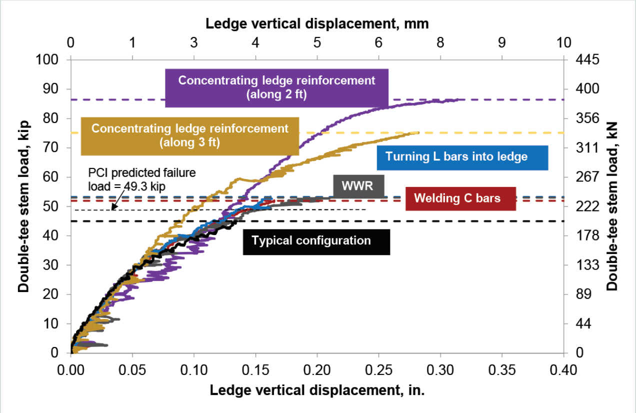

Figure 15. Ledge vertical displacements at beam end for various reinforcement details. Note: For beams with typical configuration (RS1, RS1-D), the measured concrete strength was 7310 psi (50.4 MPa), while for the rest it was 10,530 psi (72.6 MPa). WWR = welded wire reinforcement. 1 ft = 0.305 m; 1 kip = 4.448 kN.

Conclusion

Based on the findings of the short-span beams study, the following conclusions are drawn:

- The design procedure in the seventh edition of the *PCI Design Handbook* can overestimate ledge capacity, especially at midspan locations, even in the absence of high global flexural and shear stresses.

- Punching-shear failures of ledges typically initiate with diagonal cracks propagating from the back and the sides of the bearing toward the front face of the ledge followed by a sudden failure.

- The observed failure surface is larger than the surface area assumed by the PCI procedure and the failure planes typically develop at an angle shallower than the 45 degrees assumed by the PCI procedure.

- The experimental study presented indicates that four parameters significantly affect the ledge punching-shear capacity of short-span L-shaped beams: load eccentricity, concrete compressive strength, ledge height, and edge distance of the load.

- Increasing the ledge projection accompanied by increasing the load eccentricity can reduce the ledge capacity; however, if the ledge projection is increased without increasing the load eccentricity, the ledge capacity can be increased.

- The performance of four special reinforcement details considered in this study indicates the following:

  – Welding C bars to the longitudinal bottom bar in the ledge has no effect on the ledge capacity.

  – Turning the hanger reinforcement into the ledge reduces the brittleness of the failure but has a negligible effect on the ledge capacity.

  – There is no performance difference between using the welded-wire reinforcement and using the conventional ledge reinforcement, but the former is more advantageous in terms of saved fabrication time.

  – Concentrating ledge reinforcement near the applied loads can significantly enhance the ledge capacity. This option may be of use to a designer when ledge capacity must be enhanced and increases to the ledge height and/or concrete compressive strength are impractical or undesirable.

Acknowledgments

This research was sponsored by the PCI Research and Development Council. The authors are grateful to the PCI Ledge Advisory Committee for the support and guidance provided throughout the various phases of this research. The contributions by Metromont Corp. in producing test specimens for the short beams study are also gratefully acknowledged.

References

1. PCI Industry Handbook Committee. 2010. *PCI Design Handbook: Precast and Prestressed Concrete.* MNL-120. 7th ed. Chicago, IL: PCI.

2. Klein, G. J. 1986. "Design of Spandrel Beams." *PCI Journal* 31 (5): 76–124.

3. Klein, G. J. 1986. "Design of Spandrel Beams." PCI specially funded research and development program research project no. 5. Chicago, IL: PCI.

4. Hassan, T. K. 2007. "Finite Element Study of Shear Behavior of Spandrel Ledges and Comparison with PCI Shear Design Provisions." *Advances in Structural Engineering* 10 (5): 475–485.

5. Lucier, G., C. Walter, S. Rizkalla, P. Zia, and G. Klein. 2011. "Development of a Rational Design Methodology for Precast Concrete Slender Spandrel Beams: Part 1, Experimental Results." *PCI Journal* 56 (2): 88–112.

6. Lucier, G., C. Walter, S. Rizkalla, P. Zia, and G. Klein. 2011. "Development of a Rational Design Methodology for Precast Concrete Slender Spandrel Beams: Part 2, Analysis and Design Guidelines." *PCI Journal* 56 (4): 106–133.

7. Lucier, G., C. Walter, S. Rizkalla, P. Zia, and G. Klein. 2010. "Development of a Rational Design Methodology for Precast Concrete Slender Spandrel Beams." Technical report IS-09-10. North Carolina State University, Raleigh, NC.

8. Logan, D. R. 2012. "Development of a Rational Design Methodology for Precast Slender Spandrel Beams." Discussion. *PCI Journal* 57 (2): 182–187.

9. Rizkalla, S., M. Nafadi, G. Lucier, P. Zia, and G. Klein. 2016. "Behavior and Design of Directly-Loaded L-Shaped Beam Ledges." Technical report RD-16-03. North Carolina State University, Raleigh, NC.

10. Nafadi, M. K., G. W. Lucier, S. Rizkalla, P. Zia, and G. J. Klein. 2018. "Ledge Behavior and Strength of Long-Span L-shaped Beams." *PCI Journal* 63 (2): 50–66.

11. Nafadi, M. K., G. W. Lucier, S. Rizkalla, P. Zia, and G. J. Klein. 2018. "Development of Design Guidelines for Ledges of L-shaped Beams." *PCI Journal* 63 (2): 32–49.

12. PCI Industry Handbook Committee. 2017. *PCI Design Handbook: Precast and Prestressed Concrete*. 8th ed. Chicago, IL: PCI.

Notation

A_l = area of longitudinal reinforcement in ledge

A_s = area of transverse flexural reinforcement

A_{sh} = area of hanger reinforcement

b = width of web

b_l = width of web and one ledge

b_t = width of double-tee stem or bearing pad, whichever is less

d_e = distance from center of an applied concentrated load to end of ledge

DL = dead load

e' = eccentricity of ledge vertical load to the inner web face

f_c' = specified compressive strength of concrete

h = height of beam

h_l = height of beam ledge

l_b = bearing length

l_p = projection of the ledge ($b_l - b$ in section 5.5 of the seventh edition of the *PCI Design Handbook*)

LL = live load

N_{lu} = factored ledge friction load (N_u in section 5.5 of the seventh edition of the *PCI Design Handbook*)

s = spacing between applied concentrated loads

V_{ln} = nominal ledge capacity (V_n in section 5.5 of the seventh edition of the *PCI Design Handbook*)

V_{lu} = factored ledge vertical load (V_u in section 5.5 of the seventh edition of the *PCI Design Handbook*)

$V_{ln,PCI}$ = nominal ledge capacity according to section 5.5 of the seventh edition of the *PCI Design Handbook*

$V_{ln,Measured}$ = measured nominal ledge capacity

About the authors

Mohamed K. Nafadi, PhD, is an assistant professor of structural engineering at Assiut University in Assiut, Egypt. He is a former graduate research assistant in the Department of Civil, Construction, and Environmental Engineering at North Carolina State University (NCSU) in Raleigh.

Omar M. Khalafalla, is a graduate research and teaching assistant and PhD candidate in the Department of Civil, Construction, and Environmental Engineering at NCSU.

Gregory W. Lucier, PhD, is a research assistant professor in the Department of Civil, Construction, and Environmental Engineering and manager of the Constructed Facilities Laboratory at NCSU.

Sami Rizkalla, PhD, FPCI, FACI, FASCE, FIIFC, FEIC, FCSCE, is Distinguished Professor Emeritus in the Department of Civil, Construction, and Environmental Engineering at NCSU.

Paul Zia, PhD, PE, FPCI, is a Distinguished University Professor Emeritus in the Department of Civil, Construction, and Environmental Engineering at NCSU.

Gary J. Klein, PE, is executive vice president and senior principal for Wiss, Janney, Elstner Associates Inc. in Northbrook, Ill.

Abstract

The design procedure for ledges of L-shaped beams presented in the seventh edition of the *PCI Design Handbook: Precast and Prestressed Concrete* has been called into question by many engineers and researchers. Research findings from previous experimental studies have indicated that the ledge design equations provided in the seventh edition of the *PCI Design Handbook* overestimate the ledge punching-shear capacity. This paper presents the findings of the first phase of a comprehensive experimental program conducted with the objective of developing design guidelines for the ledges of L-shaped beams. In this first phase of study, short-span beams were used to minimize the effect of global stresses and the cost of testing, thus allowing for a larger number of parameters to be examined. The main objectives of this study were to investigate the ledge behavior and the configuration of the failure surface. In addition, the study also investigated the effect of various parameters believed to affect ledge behavior. The study also investigated the performance of special reinforcement details toward the development of detailing recommendations for ledge reinforcement. Research findings indicate that even with low levels of global stress, the ledge design procedure provided in the seventh edition of the *PCI Design Handbook* could overestimate the ledge capacity. Furthermore, the observed failure surface was generally larger than the assumed surface specified by the PCI procedure. The study also found that several parameters affected the ledge capacity but are not considered by the PCI procedure. Finally, the study also demonstrated that certain reinforcement details can be used to improve the ledge behavior and to enhance the ledge capacity.

Keywords

Ledge, L-shaped beams, punching shear, reinforcement details, short-span, spandrel.

Review policy

This paper was reviewed in accordance with the Precast/Prestressed Concrete Institute's peer-review process.

Reader comments

Please address any reader comments to *PCI Journal* editor-in-chief Emily Lorenz at elorenz@pci.org or Precast/Prestressed Concrete Institute, c/o *PCI Journal*, 200 W. Adams St., Suite 2100, Chicago, IL 60606.